Advances in Aircraft and Spacecraft Science, *Vol. 2, No. 4 (2015) 403-425*
DOI: http://dx.doi.org/10.12989/aas.2015.2.4.403

Analytical similitudes applied to thin cylindrical shells

Sergio De Rosa* and Francesco Franco

Pasta-Lab, Laboratory for Promoting Experiences in Aeronautical Structures and Acoustics, Department of Industrial Engineering, Aerospace Section, Università di Napoli "Federico II", Via Claudio 21, 80125 Napoli, Italy

(Received December 16, 2014, Revised January 27, 2015, Accepted February 2, 2015)

Abstract. This work is focused on the definition and the analysis of both complete and incomplete similitudes for the dynamic responses of thin shells. Previous numerical and experimental investigations on both structural and structural-acoustic systems motivated this further analysis, mainly centred on the incomplete (distorted) similitudes. These similitudes and the associated scaling laws are defined by using the classical modal approach (CMA) and by invoking also the Energy Distribution Approach (EDA) in order to take into account both the cinematic and energetic items. The whole procedure is named SAMSARA: Similitude and Asymptotic Models for Structural-Acoustic Research and Applications. A brief summary of the procedure is herein given and the attention is paid to the analytical models of thin stiffened and unstiffened cylindrical shells. By using the well-known smeared model, the stiffened cylinder equations are used as general framework to analyse the possibility to define exact (replicas) or distorted similitudes (avatars). Despite the extreme simplicity of the proposed models, the results are really encouraging. The final aim is to define equivalent models to be used in laboratory measurements.

Keywords: structural similitude; energy distribution approach; scaling laws

1. Introduction

All the researchers and analysts, involved in scientific and engineering activities, would like to work on prototypes which are able to reproduce the desired behaviour or to modify the scales of investigations. In this last case, very large models as well as very small ones could be studied at convenient sizes, hopefully keeping the original characteristics.

This is the reason for which one of the most important branches of the physics and engineering studies is related to the similitudes, that is the possibility to work on an artefact able to reproduce a given response. It is soon needed a lexical clarification: in the *similitude theory* the analyst translates the same problem on different scales whereas, within the *analogies*, a given class of problems is solved by looking for similar equations. The work by Szucs (1980) remains the main reference but further general views of both the similitude and analogies problems are also in Kline (1986), Kroes (1989).

This specific point emerges with even stronger evidence in the field of transportation engineering (naval, aerospace, civil and railway ones) where the relative importance of some

*Corresponding author, Professor, E-mail: sergio.derosa@unina.it

http://www.techno-press.org/?journal=aas&subpage=7 ISSN: 2287-528X (Print), 2287-5271 (Online)

parameters is a relevant step and thus some experimental investigations on new prototypes are highly desired, often mandatory. In this case, it would be often preferred to reduce the original sizes so that a laboratory accommodation would be more comfy.

In the literature, restricting the field to the simulation of the structural components only, it is possible to find applications related to the analysis of buckling Frostig and Simitses (2004) and the response of beams, plates and shells made of different materials, Rezaeepazhand and Yazdi (2011), Rezaeepazhand, Simitses and Starnes (1996), Rezaeepazhand (2008), Singhatanadgid and Songkhla (2008), Yazdi and Rezaeepazhand (2010).

An interesting framework for scaled models, by using the modal approach, is given in Wu (2006). In the present work, it is used a generalisation of the modal approach, the Energy Distribution Approach (EDA), Mace (2003), which allows this kind of investigation by using the classical modal approach (CMA). In fact, the mode shapes and the natural frequencies are used to determine the power input and the energy associated to each subsystem belonging to a given system. Thus, the similitude can be defined by using relationships among mode shapes, natural frequencies, damping loss factors and energies.

EDA has been already used in order to predict the original and scaled responses of linear dynamic systems. In detail, in De Rosa *et al*. (2011) the case of two plates is presented and in De Rosa *et al*. (2014) the scaling between structural components with different modal density is introduced. Recent and successful steps involved simple vibro-acoustic systems: infinite flexural cylinder/finite flexural coupled with the internal acoustics, De Rosa *et al*. (2012).

The complete procedure is named SAMSARA, *Similitude and Asymptotic Models for Structural-Acoustic Researches and Applications*.

The focus of this work is just on structural similitudes for cylindrical shells and more specifically, it is investigated the possibility to define exact and distorted similitudes and the related scaling laws for the analysis of the dynamic response.

Some highlights about the distribution of the natural frequencies and the forced response are given; further, some possibilities to assembly specific distorted models are discussed being these latter very interesting from an engineering point of view. Analytical models are used throughout the whole work for producing both the original and distorted model responses.

The results are very encouraging and they represent a good step toward the desired applications to laboratory measurements, even if the definition of SAMSARA is far to be considered a concluded topic.

The managements of the symbols is very challenging when working with this kind of problems: it is decided, here, to avoid a huge list of symbols and to introduce and define them when used in order to guarantee a continuity in the reading of the theoretical developments.

After these remarks, in Section 2, the equations are defined for both stiffened and unstiffened shells. The stiffened models refer to the well-known smeared approximation as in Mikulas and McElman (1965) and within the well-known framework defined in Leissa (1973). The same approach is used for the unstiffened case. EDA is introduced in Section 3 with some principles for defining the complete and distorted similitudes. These are fully defined in Section 4 where some choices are also presented in order to generate meaningful engineering models. The results are in Section 5 for both cases and in Section 6 some considerations are given about the overall approach and possible follow-ups. A concluding summary closes the work in Section 6.

It has to be highlighted that the work published by Torkamani *et al*. (2009) is the ideal companion of the present developments.

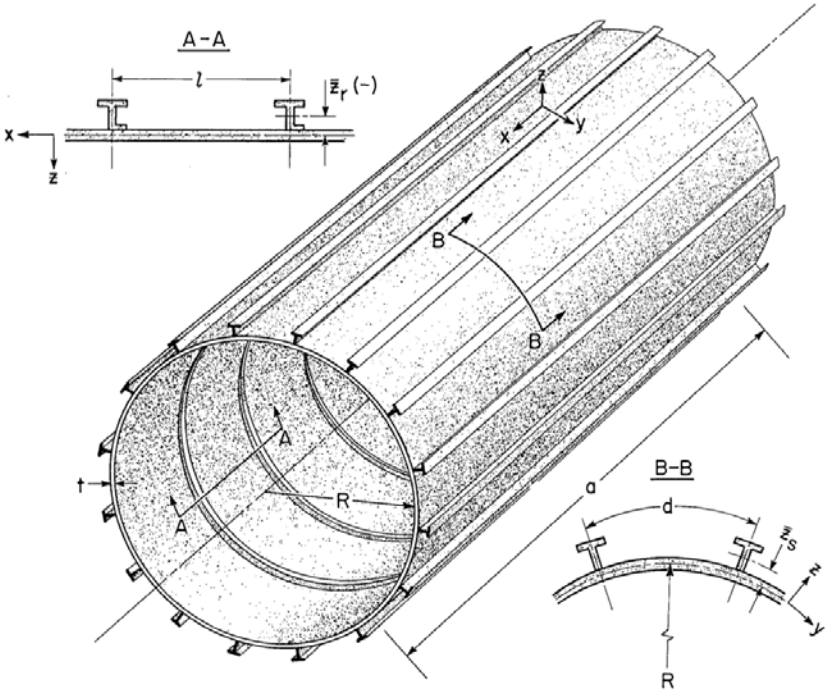

Fig. 1 Reference system for the thin shell from Mikulas and McElman (1965)

2. Cylinder response

The linear response of a thin uniform simply supported cylindrical shell can be obtained by analytical models, as reported in Mikulas and McElman (1965), Leissa (1973).

For the developments herein presented, the reference system is reported in Fig. 1, where it is considered the stiffened case. In a cylindrical reference system, the *x*-axis is the longitudinal coordinate, while *y* is the circumferential one; *z* is always oriented along the outward normal.

The bases for the associated set of displacements are *u*, *v* and *w*, respectively and they are expressed by expanding a given number of radial, *NR*, and longitudinal components, *NL*

$$u(x,y,\omega)=\sum_{n=1}^{NR}\sum_{m=1}^{NL} U(n,m,\omega)\ \cos\left(n\frac{y}{R}\right)\cos\left(m\frac{\pi x}{L}\right) \tag{1}$$

$$v(x,y,\omega)=\sum_{n=1}^{NR}\sum_{m=1}^{NL} V(n,m,\omega)\ \sin\left(n\frac{y}{R}\right)\sin\left(m\frac{\pi x}{L}\right) \tag{2}$$

$$w(x,y,\omega)=\sum_{n=1}^{NR}\sum_{m=1}^{NL} W(n,m,\omega)\ \cos\left(n\frac{y}{R}\right)\sin\left(m\frac{\pi x}{L}\right) \tag{3}$$

where *R* and *L* are the symbols for the radius and the length of the cylinder.

The general structural solutions can be found by using the Donnell-Mushtari equations, $\mathbf{L}_{DM}(\omega)$

with or without some modifiers, $\mathbf{L}_{MOD}(\omega)$, which can refine the representation by adopting an improved stress-strain state, Leissa (1973).

In terms of operators

$$\left[\mathbf{L}_{DM}(\omega)+\frac{h^2}{12R^2}\mathbf{L}_{MOD}(\omega)\right]\begin{Bmatrix}u(x,y,\omega)\\ v(x,y,\omega)\\ w(x,y,\omega)\end{Bmatrix}=\begin{Bmatrix}F_x(x_F,y_F,\omega)\\ F_y(x_F,y_F,\omega)\\ F_z(x_F,y_F,\omega)\end{Bmatrix} \tag{4}$$

where h is the thickness of the shell; $\mathbf{F}$ is a generic excitation vector acting at the point $P_F(x_F, y_F)$. It is preferred here to give the due detail to the operator as defined in Mikulas and McElman (1965), directly referring to the orthogonally stiffened cylinder, named $\left[\mathbf{L}^{(s)}(\omega,m,n)\right]$

$$\left[\mathbf{L}^{(s)}(\omega,m,n)\right]=\begin{bmatrix}-[1+SS(1-\nu^2)+\beta^2(\frac{1-\nu}{2}) & -\frac{1+\nu}{2} & \mu+(1-\nu^2)\alpha^2 SS\frac{z_S}{R}\\ -\frac{1+\nu}{2} & -[1+RR(1-\nu^2)+\frac{1-\nu}{2\beta^2}] & 1+RR(1-\nu^2)(1+n^2\frac{z_R}{R})\\ \nu+(1-\nu^2)\alpha^2 SS\frac{z_S}{R} & 1+RR(1-\nu^2)(1+n^2\frac{z_R}{R}) & L_{3,3}^{(s)}\end{bmatrix} \tag{5}$$

where the following dimensionless groups are usually defined

$$\beta=\frac{nL}{m\pi R};\ \alpha=\frac{m\pi R}{L} \tag{6}$$

$$SS=\frac{E_S A_S}{Ehd};\ RR=\frac{E_R A_R}{Ehl} \tag{7}$$

The term α is often indicated as Λ. The pedices S and R denote properties belonging to circumferential and radial stiffeners, respectively; E, E_S and E_R are the normal elasticity modules; D is the flexural stiffness; G, G_S and G_R are the shear elasticity modules; ν is the Poisson elasticity module; I_S, I_R, J_S and J_R are the inertia moments; ρ, ρ_S and ρ_R are the mass densities; l and d are the spacing among longitudinal and radial stiffeners (Fig. 1); z_S and z_R are the distances of centroids of the stiffeners from the middle surface of the shell; A_S and A_R are the section areas of the stiffeners.

The term $L_{33}^{(s)}$ is rather complicated

$$\begin{aligned}L_{3,3}^{(s)}=&-\frac{D\alpha^4(1-\nu^2)(1+\beta^2)^2}{E\,h\,R^2}-1-RR\,(1-\nu^2)+\frac{M^{(s)}\omega^2R^2(1-\nu^2)}{E\,h}-\frac{E_S\alpha^4(1-\nu^2)(I_S+z_S^2A_S)}{R^2\,d\,E\,h}+\\&-\frac{E_Rn^4(1-\nu^2)(I_R+z_R^2A_R)}{R^2\,l\,E\,h}-2RR\,n^2\frac{z_R}{R}(1-\nu^2)+\left[\frac{G_SJ_S}{d}+\frac{G_RJ_R}{l}\right]\left[\frac{\alpha^2n^2(1-\nu^2)}{E\,h\,R^2}\right]\end{aligned} \tag{8}$$

The mass per unit area is $M^{(s)}=\rho h+\rho_S\frac{A_S}{d}+\rho_R\frac{A_R}{l}$.

It is useful to rewrite the operator for the unstiffened case by simply eliminating the presence of

the stiffening members in Eq. (5)

$$\left[\mathbf{L}^{(u)}(\omega,m,n)\right]=\begin{bmatrix} -1+\beta^2\left(\frac{1-\nu}{2}\right) & -\frac{1+\nu}{2} & \nu \\ -\frac{1+\nu}{2} & -\left[1+\frac{1-\nu}{2\beta^2}\right] & 1 \\ \nu & 1 & L_{3,3}^{(u)} \end{bmatrix} \tag{9}$$

Even the term $L_{3,3}^{u}$ is simplified

$$L_{3,3}^{(u)}=-\frac{D\alpha^4(1-\nu^2)(1+\beta^2)^2}{E\,h\,R^2}-1+\frac{M^{(u)}\omega^2R^2(1-\nu^2)}{E\,h} \tag{10}$$

being $M^{(u)}=\rho h$. It has to be noted that the operators in Eq. (5) and Eq. (9) are both symmetrical.

More refined models can be computed by introducing the inertial effects, $\frac{M^{(s)}\omega^2R^2(1-\nu^2)}{E\,h}$ not only in the radial degrees of freedom but also in the longitudinal and tangential ones. This choice leads to a complicated interlacing of modes for each frequency. For the unstiffened case, this is well reported and discussed in del Rosario and Smith (1996). This refinement of the models is not relevant for the present developments and thus it is neglected.

The analysis of the determinants of the problems in Eq. (5) and Eq. (9) allows determining the natural frequencies of the related operators. Thus, looking for similitude models means as first step to find the sets of parameters, which are able to get the same or scaled eigenfrequencies.

It is easy to demonstrate that for stiffened cylinder, the definition of an exact similitude needs 16 conditions as reported in Torkamani *et al*. (2009). These become 14 when neglecting the in-plane stress (N_x, N_y). For the unstiffened cylinder, Eq. (9), they are 6.

The fulfilment of the 14 (or 6) conditions generates a new cylinder that exactly replicates the natural frequencies of the original model. If only one condition is violated, the new cylinder reproduces the natural frequencies in an approximated way.

The cited conditions of perfect similitude are herein reported, by noting also that the symbol $\bar{g}$ is the parameter g in similitude and the associated scaling law is $r_g=\frac{\bar{g}}{g}$. In both the cases, the similitudes of the natural frequencies have to be discussed according with the chosen set of parameters and thus is not reported in these initial sets.

For the stiffened case

$$\begin{cases} r_n=1 & r_m=1 & r_\nu=1 & r_m r_R r_L^{-1}=1 & r_h^{-1}r_R^{-1}r_L^2=1 \\ r_{z_R}r_R^{-1}=1 & r_{E_S}r_{I_S}r_D^{-1}r_d^{-1}=1 & r_{E_R}r_{I_R}r_D^{-1}r_l^{-1}=1 & r_{E_S}r_{A_S}r_E^{-1}r_h^{-1}r_d^{-1}=1 & \\ r_{z_S}r_R^{-1}=1 & r_{G_S}r_{J_S}r_D^{-1}r_d^{-1}=1 & r_{G_R}r_{J_R}r_D^{-1}r_l^{-1}=1 & r_{E_R}r_{A_R}r_E^{-1}r_h^{-1}r_l^{-1}=1 & \end{cases} \tag{11}$$

For the unstiffened case

$$\begin{cases} r_n = 1 \\ r_m = 1 \\ r_v = 1 \\ r_m r_R r_L^{-1} = 1 \\ r_h^{-1} r_R^{-1} r_L^2 = 1 \end{cases} \tag{12}$$

At this point to avoid confusion, it is necessary to introduce and define two terms.

It is intended as a *replica* a new cylinder that fulfils all the similitude conditions. In this case, it will be shown that all the natural frequencies are scaled by the same parameter: a *replica* represents an exact similitude.

A distorted similitude, a situation in which at least one of the parameters is not perfectly scaled is named as *avatar*. The main attention of the work is just on the definition of some *avatars*, since the *replicas* could be very difficult to obtain, as later shown.

It has to be also highlighted that the natural frequencies are only a part of the response problem. A full set of parameters is so needed in order to guarantee that the replicas and/or the avatars allow reading also the response and to this aim EDA is invoked.

3. Summary of energy distribution approach (EDA)

Full similitudes can be defined by invoking the energy distribution approach, a tool that represents a starting point for defining the needed parameters.

3.1 Background

A generic linear structural-acoustic dynamic model can be assembled by using the mode shapes and natural frequencies: with these information, the distribution of energy in each subsystem can be obtained, being a subsystem defined as a spatial domain characterised by specific waves. Thus, the whole system can be thought as an assembly of *NS* subsystems in which *NM* modes are resonating at each excitation frequency.

Through the energy influence coefficient matrix, $\mathbf{A}^{\mathbf{EIC}}$ it is possible to estimate the energy unknown vector, $\mathbf{E}$, for a given power input vector, $\mathbf{P}_{\mathbf{input}}$

$$\mathbf{E}(\Omega) = \mathbf{A}^{EIC}(\Omega)\mathbf{P}_{\mathbf{input}}(\Omega) \tag{13}$$

with

$$A_{rq}^{EIC}(\Omega) = \frac{\sum_j \sum_k \Gamma_{jk}(\Omega)\psi_{jk}^{(q)}\psi_{jk}^{(r)}}{\sum_j \eta_j \Omega_j \Gamma_{jj}(\Omega)\psi_{jj}^{(q)}} \; with \;\; r,q \in \{1,\ldots NS\} j,k \in \{1,\ldots NM\} \tag{14}$$

EDA allows the estimation of such matrix, $\mathbf{A}^{EIC}$. The spatial coupling parameter for the generic *r*-th subsystem is the following

$$\psi_{jk}^{(r)} = \int_{\mathbf{x}\in r} \rho(\mathbf{x})\phi_j(\mathbf{x})\phi_k(\mathbf{x})d\mathbf{x} \tag{15}$$

Here, the term **x** denotes the generic spatial dependence. The $\psi_{jk}^{(r)}$ depends on the interaction between the global mode shapes, φ_j and φ_k, when acting within the *r*-th subsystem. The global mode shapes are considered mass-normalized: the ψ_{jk} terms are dimensionless.

The frequency dependent members are here recalled

$$\Gamma_{jk}(\Omega) = \frac{1}{\Omega}\int_{\omega\in\Omega} \omega^2 Re\left[\alpha_j(\omega)\alpha_k(\omega)\right]\, d\omega \tag{16}$$

where the modal frequency dependent receptance for the *j*-th mode α_j is given by

$$\alpha_j(\omega) = \frac{1}{\omega_j^2 - \omega^2 + iu\,\eta_j\omega_j^2} \tag{17}$$

The terms Ω and ω represent generic frequency interval and excitation frequency, respectively; the ω_j and η_j are the natural frequencies and the associated modal damping. The imaginary unit is iu. Ω is the interval in which the system response is analysed for a given excitation.

The generic cross-modal term, Γ_{jk}, is a frequency integral whose magnitude depends primarily on the natural frequencies and the bandwidths of the *j*-th and *k*-th modes. For small damping, the modal terms can be approximated, (Mace 2003); the auto terms

$$\Gamma_{jj}(\Omega) \cong \frac{1}{8\Omega}\frac{\pi}{\eta_j\omega_j} \tag{18}$$

and the cross terms

$$\Gamma_{jk}(\Omega) \cong \frac{\pi}{16\Omega}\frac{\left(\omega_j+\omega_k\right)^2\left(\eta_j\omega_j+\eta_k\omega_k\right)}{\left(\omega_j^2-\omega_k^2\right)^2+\left(\eta_j\omega_j^2+\eta_k\omega_k^2\right)^2} \tag{18}$$

The analysis of the cross terms is rather complicated and two further approximations can be used that allow separating the cross terms in large and small terms

$$\Gamma_{jk}^{(large)}(\Omega) \cong \frac{\pi}{16\Omega}\frac{\left(\omega_j+\omega_k\right)^2\left(\eta_j\omega_j+\eta_k\omega_k\right)}{\left(\eta_j\omega_j^2+\eta_k\omega_k^2\right)^2} \tag{19}$$

$$\Gamma_{jk}^{(small)}(\Omega) \cong \frac{\pi}{16\Omega}\frac{\left(\omega_j+\omega_k\right)^2\left(\eta_j\omega_j+\eta_k\omega_k\right)}{\left(\omega_j^2-\omega_k^2\right)^2} \tag{20}$$

In EDA, the loading is assumed to be proportional to mass density with zero cross-spectral density, S_f, further, it has to be noted that the units are such that $[S_f]=[F\ LT^{-1}]$. The expressions of the input power, *P* into to the *q*-th subsystem and the kinetic energy, *T*, for the *r*-th one subsystem, do complete the dynamic set for the analysis

$$P_{input}^{(q)}\left(\Omega\right)=2S_f\sum_j 2\eta_j\omega_j\Gamma_{jj}\left(\Omega\right)\psi_{jj}^{(q)}$$
$$T^{(r)}\left(\Omega\right)=2S_f\sum_j\sum_k\Gamma_{jk}\left(\Omega\right)\psi_{jk}^{(q)}\psi_{jk}^{(r)} \tag{22}$$

3.2 Similitude

It is possible to study any similitude by looking at the variation of the main parameters defined in EDA: Γ involves the natural frequencies and the damping; the ψ involve the global mode shapes; S_f involves the spectrum of the excitation and the mass of the system.

It is useful to highlight the working hypotheses:

1. The material constants do not change in the replicas and avatars: any material variation can be interpreted as a modification in the distribution of the natural frequencies.
2. The boundary conditions remain the same in the replicas and avatars.
3. The global mode shapes remain unaffected: $\phi_j=\bar{\phi}_j$; as consequence, one gets that the scaled spatial coupling parameters are equal to the original ones: $\overline{\psi}_{jk}^{(\bar{r})}=\psi_{jk}^{(r)}$.
4. The structural excitations are concentrated harmonic forces acting at the point generic point P_F and time t: $f(P,\omega)=F(\omega)\delta(P-P_F)$.
5. The system response is obtained by using real mode shapes and natural frequencies.

It is desired to have variations of these latters, which can be re-modulated in a univocal way so that from the replicas or avatars one can recover the original response.

The scaled auto and cross-modal frequency response operators are here defined without further details and by invoking directly the approximations for the small damping (for the sake of brevity the Ω dependence has also omitted)

$$\bar{\Gamma}_{jj}=\frac{1}{r_\eta r_\omega^2}\Gamma_{jj} \tag{23}$$

$$\bar{\Gamma}_{jk}^{(large)}=\frac{1}{r_\eta r_\omega^2}\Gamma_{jk}^{(large)} \tag{24}$$

$$\bar{\Gamma}_{jk}^{(small)}=\frac{r_\eta}{r_\omega^2}\Gamma_{jk}^{(small)} \tag{25}$$

The excitation is scaled according to its units

$$\bar{S}_f=S_f\frac{r_f^2}{r_{mass}} \tag{26}$$

Through EDA, the relevant scaling laws according to the previous hypotheses are: the natural frequencies, $r_\omega=\frac{\bar{\omega}_j}{\omega_j}$, the damping, $r_\eta=\frac{\bar{\eta}}{\eta}$, the excitation spectrum, $r_F=\frac{\bar{F}}{F}$ and the structural mass being: $r_{mass}=\frac{\bar{M}}{M}$.

For the sake of completeness, it is useful to list all the remaining EDA parameters when approached with the scaling procedure

$$\begin{aligned} \bar{P}_{IN}^{(q)} &= P_{IN}^{(q)} \frac{r_f^2}{r_\omega r_m} \\ \bar{T}^{(r)} &= T^{(r)} \frac{r_f^2}{r_m r_\omega^2 r_\eta} \end{aligned} \tag{27}$$

The effect of a given damping modification on the parent models can be observed from Eqs. (23), (24) and (25). The role of the cross modal terms is not exactly reproduced if $r_\eta \neq 1$, even for the same distribution of the natural frequencies. This has been already studied and discussed for a number of cases, De Rosa *et al*. (2011, 2012).

It can be stated now that

$r_\eta \neq 1$: it is impossible to get a replica but only avatars;

$r_\eta = 1$: replicas do exist and can be found.

4. Analysis of shells

It is useful to underline again that as engineering choice, in all this work, it is decided to keep the original material constants even in the parent models. In principle, it is possible to include also this further degree of freedom but this can lead to a huge subset of parameters to be taken into account and/or to mathematical solution impossible to replicate in a lab. In any case all the material variations can be interpreted as a modification in the distribution of the natural frequencies.

4.1 Unstiffened

In the present development, the cylinder is studied adopting as set of geometrical parameters the length, the radius and the thickness (L, R and h), respectively[1], Fig. 1.

Thin shells represent the models under investigations and thus it is assumed that $\frac{h^2}{12R^2} << 1$.

The field of investigation is restricted to the analysis of the influence of the geometrical parameters and the force one, F: a similitude has been searched with this following a set of parameters

$$r_L = \frac{\bar{L}}{L},\ r_h = \frac{\bar{h}}{h},\ r_R = \frac{\bar{R}}{R},\ r_F = \frac{\bar{F}}{F} \tag{28}$$

Another key parameter is the ratio of the natural frequencies, which is derived according with the other ones

$$r_\omega = \frac{\bar{\omega}_j}{\omega_j} \tag{29}$$

[1]Here it is preferred L rather than a as symbol for the length.

The condition of a perfect similitude in the present hypotheses can be written as follows

$$\begin{cases} r_n = 1 \\ r_m = 1 \\ r_m r_R r_L^{-1} = 1 \\ r_h^{-1} r_R^{-1} r_L^2 = 1 \end{cases} \tag{30}$$

It has to remembered that:

(i) the terms *m* and *n* are the mode indexes, Eqs. (1)-(3); the first and second relations preserve the sequence on the modes in both the original cylinder and replicas/avatars;

(ii) the third relation expresses the parameter $\Lambda = \frac{m\pi R}{L}$ (the alpha in Eq. (6));

(iii) the fourth allows keeping the parameter $\Pi = \frac{Rh}{L^2}$.

The first two conditions are respected in any case since the analytical modal expansions are interrogated for any of *mn*-th structural mode. The natural frequencies remain to be discussed.

In Torkamani *et al*. (2009) they are assumed such as $r_\omega = r_h r_L^{-2}$, but they represent a very simplified model. In Blevins (1987), the natural frequencies for a thin simply supported cylindrical shell without axial constraints are simplified and classified as: torsion, axial, radial, bending and axial-radial modes. All the natural frequencies scale with r_R, that is

$$r_\omega = r_R^{-1} \tag{31}$$

with the only exception of the axial-radial ones which - under the hypothesis $\left(\frac{m\pi R}{L}\right)^2 << n^2$ - can be written as

$$\omega_{m,n} = \frac{\sqrt{\frac{E}{\rho(1-\nu^2)}\left[\left(1-\nu^2\right)\left(\frac{m\pi R}{L}\right)^4 + \frac{h^2}{12R^2}\left(\frac{m^2\pi^2R^2}{L^2}+n^2\right)^4\right]}}{R\left[\left(\frac{m\pi R}{L}\right)^2 + n^2\right]} \tag{32}$$

These are the distorted natural frequencies

$$\overline{\omega}_{m,n} = \frac{\sqrt{\frac{E}{\rho(1-\nu^2)}\left[\left(1-\nu^2\right)\left(\frac{m\pi R}{L}\right)^4 \frac{r_R^4}{r_L^4} + \frac{r_h^2}{r_R^2}\frac{h^2}{12R^2}\left(\frac{m^2\pi^2R^2}{L^2}\frac{r_R^2}{r_L^2}+n^2\right)^4\right]}}{r_R R\left[\left(\frac{m\pi R}{L}\right)^2 \frac{r_R^2}{r_L^2} + n^2\right]} \tag{33}$$

It has to be highlighted that in Eqs. (32) and (33) the modes with n=1 and a generic m are the pure bending modes.

A complete similitude of the original cylinder, a *replica*, can be obtained by simply selecting $r_h = r_L = r_R$. In this way, all the conditions are satisfied and the natural frequencies r_ω scaled as r_r^{-1}.

This a trivial combination, since the larger (or smaller) cylinder can be rather difficult (or impossible) to manufacture due to the thickness values in the replicas.

Thus, it would be highly efficient to look for an *avatar*, that is a model in which some relaxations in similarity conditions can be applied in order to get a good parent on which perform measurements and/or evaluations.

A generic *avatar* can be thought as obtained with three different values of the three geometrical parameters. This is associated to a superposition of the longitudinal and radial waves completely different from the original one. In general, they could not be useful for engineering purposes, but it is later discussed a specific case when the three different values are close to a replica.

A more useful combination can be obtained by imposing that: $r_L=r_R$. This is a good engineering set of parameters in view of Eq. (33) and one gets

$$\begin{cases} r_m = r_n = 1 \\ r_R = r_L \\ r_R \neq r_h \end{cases} \tag{34}$$

The third condition is a violation of the complete similitude and this expresses the distortion of the *avatar*: the dimensionless parameters Π and $\overline{\Pi}$ are not the same. Thus, the *avatar* cylinder, can be used only in the frequency range where the couple of wave-forms allows the following condition

$$\left(1-\nu^2\right)\cdot\left(\frac{m\pi R}{L}\right)^4 >> \frac{h^2 r_h^2}{12R^2 r_R^2}\left(\frac{m^2\pi^2R^2}{L^2}+n^2\right)^4 \tag{35}$$

In this case the *avatar* is a good approximated model for representing the original cylinder being valid Eq. (31).

Thanks to EDA is thus possible to build a similitude for any choice of scaling laws. Table 1 just reports one of this for a specific combination.

In the present developments, the condition $r_\eta=1$ is preserved in order to reduce the possible variation of the avatars and again, to avoid situation in which experimentally difficulties could be hard to manage.

Table 1 Similitude parameters r_L, r_R, r_h and r_F

Conditions: $r_L=r_R$ and $r_\eta=1$		
natural frequencies		$r_\omega \approx r_R^{-1}$
mass		$r_M = r_R^2\ r_h$
frequency terms	Eq. (23), (24), (25)	$r_\Gamma \approx r_R^2$
spectral density	Eq. (26)	$r_S = r_F^2\ r_R^{-2}\ r_h^{-1}$
input power	Eq. (27)	$r_P \approx r_F^2\ r_R\ r_h^{-1}$
energies	Eq. (27)	$r_T \approx r_F^2\ r_h^{-1}$
response	$\nu^2 \propto \frac{T}{M}$	$r_{sr} \approx r_F^2\ r_R^2$

Now, an *avatar* response can be fully defined by using the contents similar to Table 1, which reports the most important parameters for the elastic response and the related scaling laws. The parameters allow re-modulating the response from the avatars (or replicas) to the original ones, since the scaling laws, r, represent the constants to be used to recover the investigated original response.

4.2 Stiffened

The main choice for the stiffened cylinder is again to keep the same materials and damping constants. The condition of perfect similitudes simplifies as follows

$$\begin{cases} r_n = 1 & r_m = 1 & r_h^{-1} r_R^{-1} r_L^2 = 1 & r_m r_R r_L^{-1} = 1 \\ r_{z_R} r_R^{-1} = 1 & r_{I_S} r_D^{-1} r_d^{-1} = 1 & r_{I_R} r_D^{-1} r_l^{-1} = 1 & r_{A_S} r_h^{-1} r_d^{-1} = 1 \\ r_{z_S} r_R^{-1} = 1 & r_{J_S} r_D^{-1} r_d^{-1} = 1 & r_{J_R} r_D^{-1} r_l^{-1} = 1 & r_{A_R} r_h^{-1} r_l^{-1} = 1 \end{cases} \tag{36}$$

The discussion here is much more complicated even working with the set of Eq. (36). In fact, the avatars can be built by using different scaling laws for each class (longitudinal and circumferential) and this can be made independently from the skin length, radius and thickness. From an engineering point of view rather than investigate the possible solutions in similitude of the determinant in Eq. (5), together with conditions in Eq. (36) respected or violated, it is preferred to work directly with engineering acceptable solutions. These are discussed in Section 5.2.

5. Results

It is useful to report the main parameters used for the numerical interrogations of the test case. The number of the radial components has been set to NR=18; the longitudinal are NL=18, too. The structural damping is assumed constant, η=0.02. All the cylinders are made in aluminium: E=70 GPa, ν=0.33, ρ=2750 kg m^{-3}.

The white-noise structural excitation is located at $x=L/4$ and $y=\pi R/4$. The force components are $F_y=F_z=1$. The response is acquired at $x=L/7$ and $y=\pi R/3$.

5.1 Unstiffened shell

Three unstiffened cylinders are considered and their sizes are in Table 2. The choice of these is made in order to take into account the variations of the main dimensionless groups (Λ and Π).

Table 2 Main geometrical and dimensionless parameters

Cylinder	L	R	h	Λ (m=1)	Π
A	10 m	1 m	1 mm	π 0.1	10^{-5}
B	10 m	2 m	1 mm	π 0.2	2 10^{-5}
C	5 m	2 m	1 mm	π 0.4	8 10^{-5}

Table 3 Unstiffened avatars

Avatars	r_L	r_R	r_h	Λ (m=1)	Π	*Figure*
A-Av$_1$	0.5	0.5	1	π 0.1	2 10^{-5}	2
A-Av$_2$	0.3	0.3	1	π 0.1	3.33 10^{-5}	3
A-Av$_3$	0.3	0.4	0.5	π 0.133	2.22 10^{-5}	4
B-Av$_1$	0.5	0.5	1	π 0.2	4 10^{-5}	5
B-Av$_3$	0.3	0.4	0.5	π 0.2667	4.44 10^{-5}	6
C-Av$_1$	0.5	0.5	1	π 0.4	16 10^{-5}	7
C-Av$_3$	0.3	0.4	0.5	π 0.533	17.76 10^{-5}	8

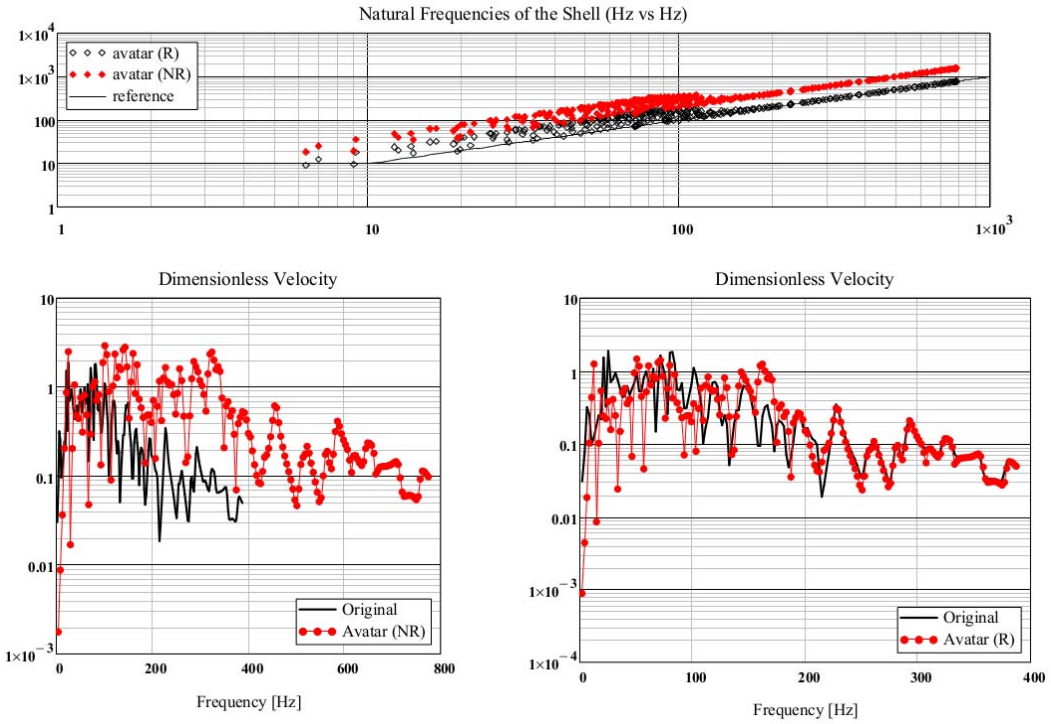

Fig. 2 Unstiffened cylinder (L=10 m, R=1 m, h=1 mm, r_L=r_R=0.5, r_h=1); upper figure: natural frequencies, lower left and right parts: comparisons of the forced responses; avatar: A-Av$_1$

The list of avatars is reported in Table 3, which includes the scaling laws, the Λ and Π dimensionless groups and the Figures related to the results. In the avatars, the first letter of the acronyms refers to the original cylinder and the last digit denotes the set of scaling laws.

Each figure of the set related to the unstiffened cylinders presents three charts. The top is related to the distribution of the natural frequencies in the original and avatar configurations before and after the re-modulation with r_ω. The horizontal axis reports for the first 324 modes (combination of 18 radial and 18 longitudinal) the original natural frequencies; the vertical axis reports the *avatar* ones, after re-modulating them. It has be highlighted that the distortion results not only in an alteration of the natural frequencies, but in their sequence too.

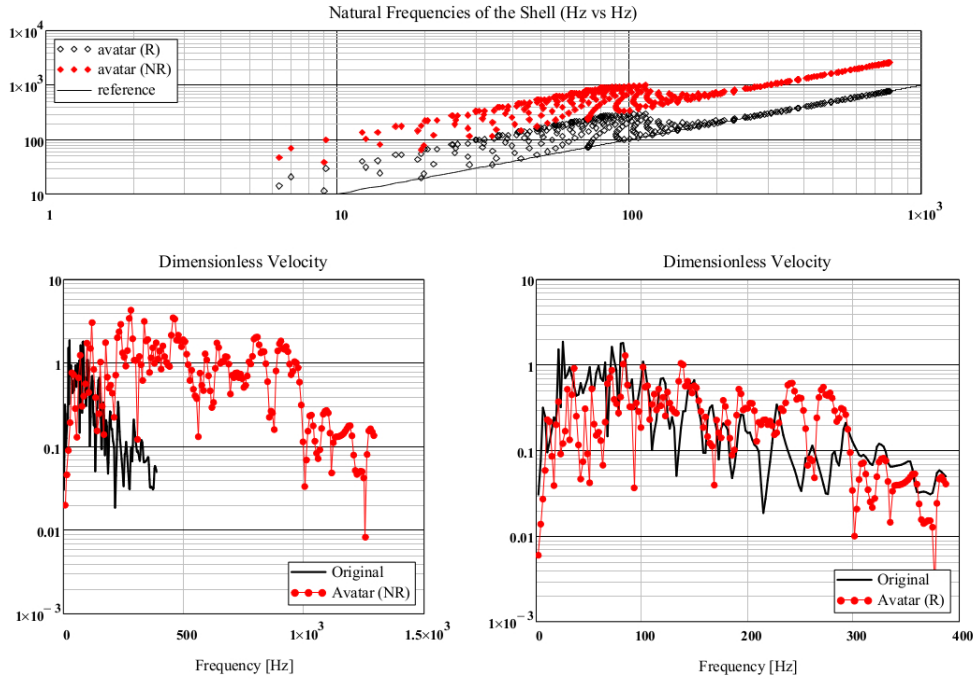

Fig. 3 Unstiffened cylinder (L=10 m, R=1 m, h=1 mm, r_L=r_R=0.3, r_h=1); upper figure: natural frequencies, lower left and right parts: comparisons of the forced responses; avatar: A-Av$_2$

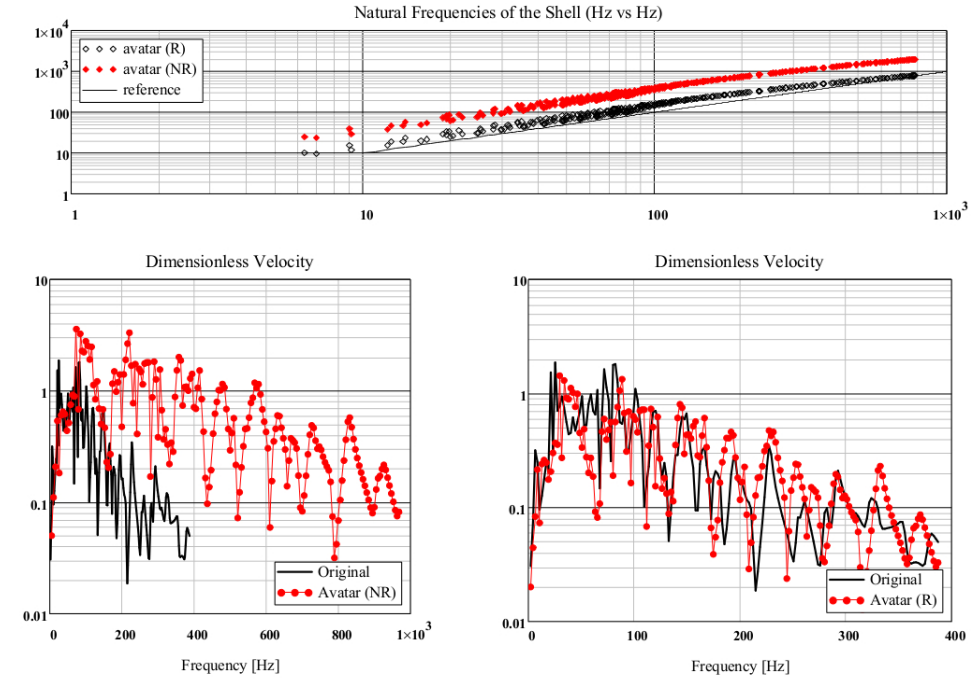

Fig. 4 Unstiffened cylinder (L=10 m, R=1 m, h=1 mm, r_L=0.3, r_R=0.4, r_h=0.5); upper figure: natural frequencies, lower left and right parts: comparisons of the forced responses; avatar: A-Av$_3$

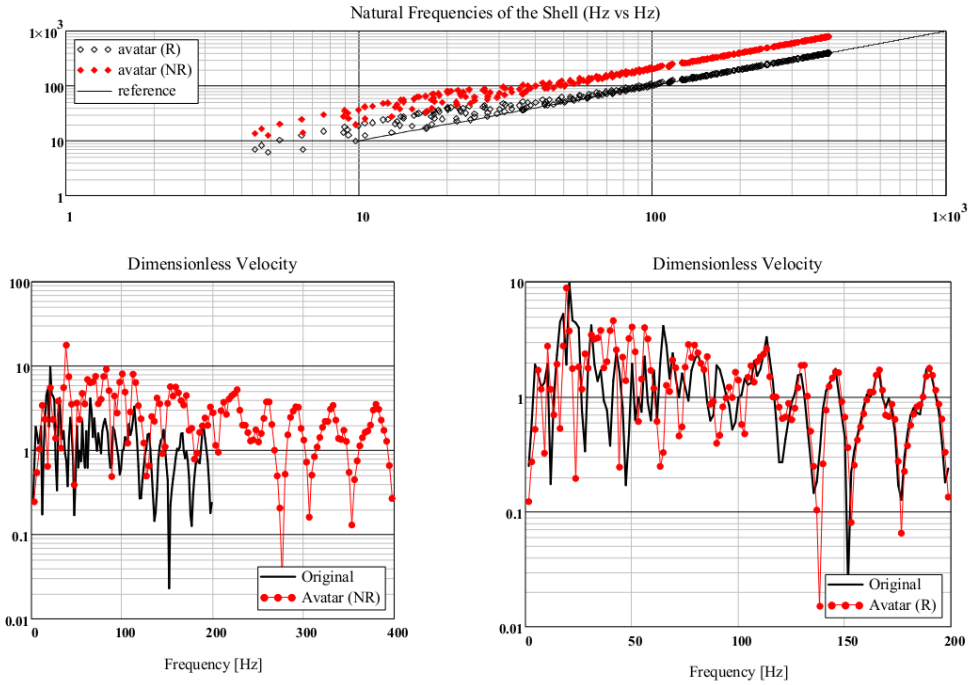

Fig. 5 Unstiffened cylinder (L=10 m, R=2 m, h=1 mm, r_L=0.5, r_R=0.5, r_h=1); upper figure: natural frequencies, lower left and right parts: comparisons of the forced responses; avatar: B-Av$_1$

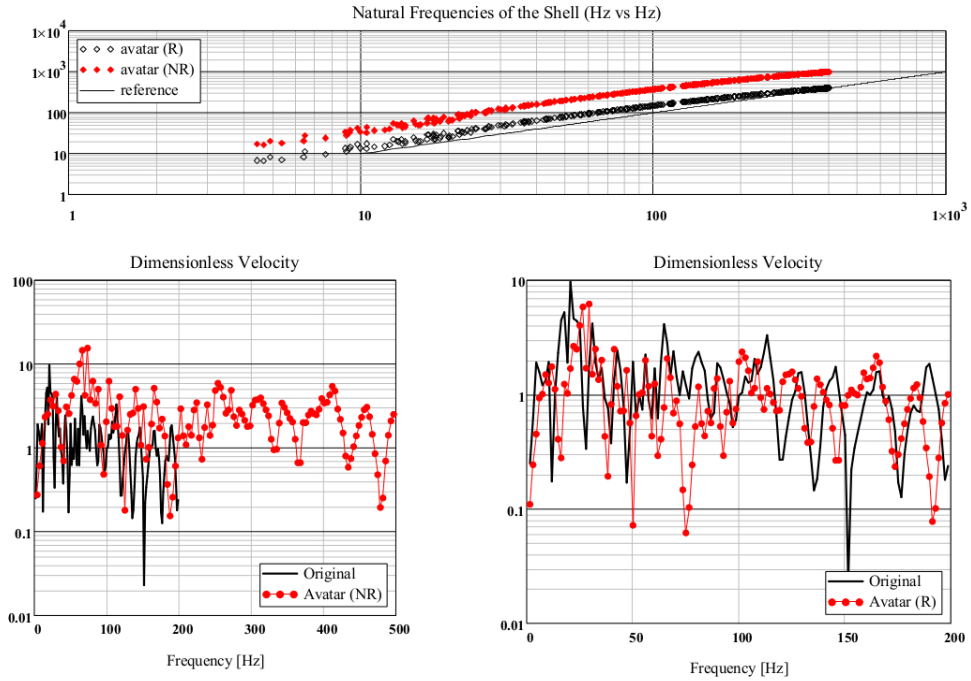

Fig. 6 Unstiffened cylinder (L=10 m, R=2 m, h=1 mm, r_L=0.3, r_R=0.4, r_h=0.5); upper figure: natural frequencies, lower left and right parts: comparisons of the forced responses; avatar: B-Av$_2$

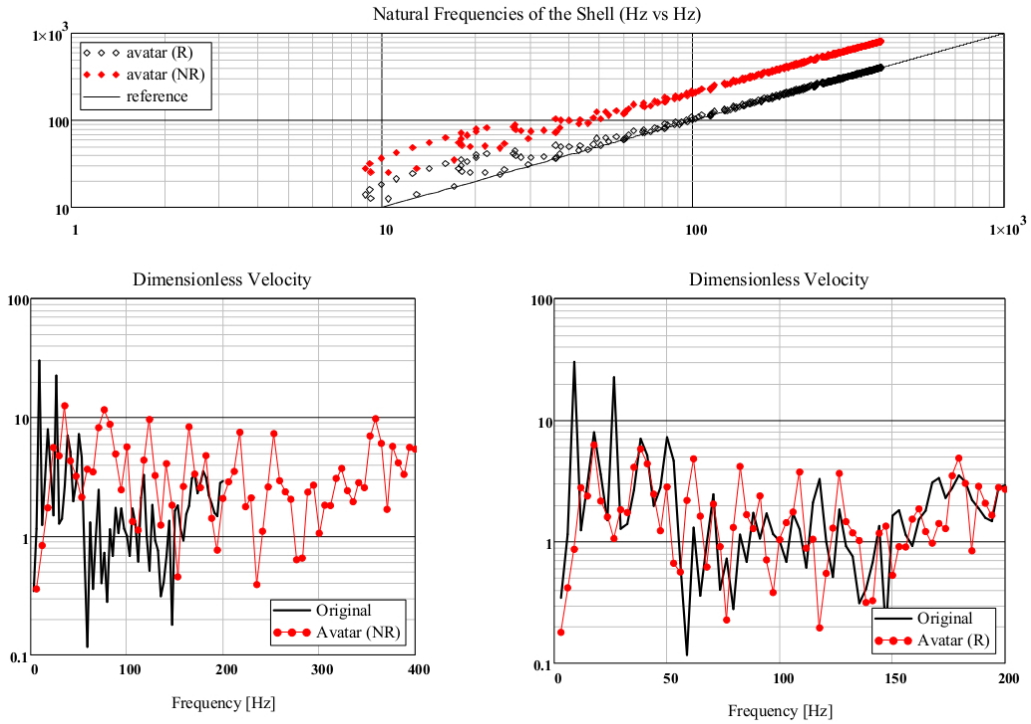

Fig. 7 Unstiffened cylinder (L=5 m, R=2 m, h=1 mm, r_L=0.5, r_R=0.5, r_h=1); upper figure: natural frequencies, lower left and right parts: comparisons of the forced responses; avatar: C-Av$_1$

For this specific item, Eq. (32) and Eq. (33) should be analysed. In fact, the proposed avatars do not alter the original distribution only when r_L=r_R=r_h; this is the generation of the replicas and this case is not discussed here.

In case of r_h=1, the natural frequencies are well reproduced according to the condition in Eq. (35). Figs. 2, 3, 5 and 7 present just these cases in which above a limit frequency, the avatars well replicate the original natural frequencies. The diagonal of these log-log charts is reported for the sake of convenience. In all other cases, the distortions are greater then the case of r_h=1 and they are rather also difficult to interpret.

For all the numerical interrogations concerning the modal expansion, the same convergence is guaranteed for all the models (original and avatars). This is well visible in the lower left charts of each figure. There, the original and avatar responses are plotted together without any scaling law corrections and therefore they work in different frequency ranges.

The lower right parts of each figure report the original and avatar responses after re-modulating this latter with the scaling laws.

The analysis of the responses starts involving the avatars A-Av$_1$, B-Av$_1$ and C-Av$_1$: in fact, the y-axes have the same scaling laws. They all present a frequency, which discriminates the applicability of the avatars as before mentioned for the natural frequencies. Among them, the A-Av$_1$ is the best of the group since its response is related to the most slender one. Furthermore, the distortions of both Λ the Π parameters are the smallest. In the responses, one can easily find the results of these considerations, being the C-Av1 the worst of the group.

The A-Av$_2$, Fig. 3, presents a huge distortion since r_L=r_R=0.3 and thus the avatar reproduces the original response at frequency higher than the interval assured by the given number of modes.

The most interesting group is A-Av$_3$, B-Av$_3$ and C-Av$_3$. In fact, in principle they are associated with high degree of variation of the original cylinders, but at the same time they are very close to a replica (r_L=r_R=r_h). Again in this group, C-Av$_3$ is the worst for the reasons already discussed.

5.2 Orthogonally stiffened shell

To take into account the stiffened cylinders, the configurations under investigation are the same as Table 2. In this case, a presence of *NCR* longitudinal and *NCL* circumferential stiffeners. They are set to *NCR*=8 and *NCL*=20. The stiffeners material is aluminium, too. The section of these beams is rectangular and the areas are 12×17 mm^2 and 10×15 mm^2, longitudinal and circumferential values respectively.

Table 4 Stiffened avatars

Avatars	r_L	r_R	r_h	*Figure*
A-Av$_1$S	0.5	0.5	1	9
A-Av$_2$S	0.2	0.2	1	10
A-Av$_3$S	0.4	0.3	0.5	11
B-Av$_1$S	0.5	0.5	1	12
C-Av$_1$S	0.5	0.5	1	13

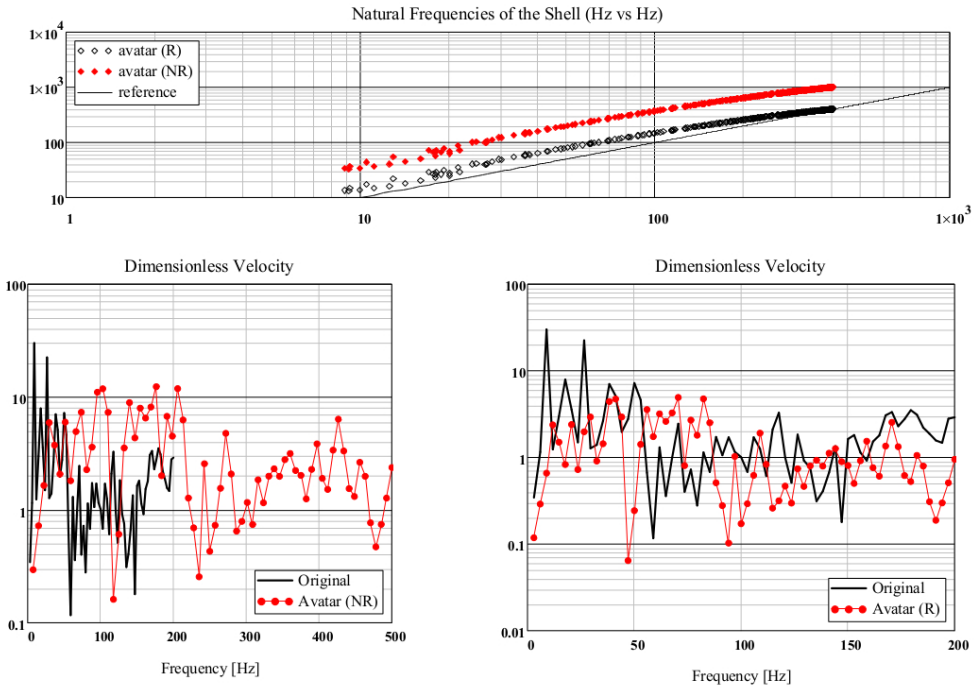

Fig. 8 Unstiffened cylinder (L=5 m, R=2 m, h=1 mm, r_L=0.3, r_R=0.4, r_h=0.5); upper figure: natural frequencies, lower left and right parts: comparisons of the forced responses; avatar: C-Av$_2$

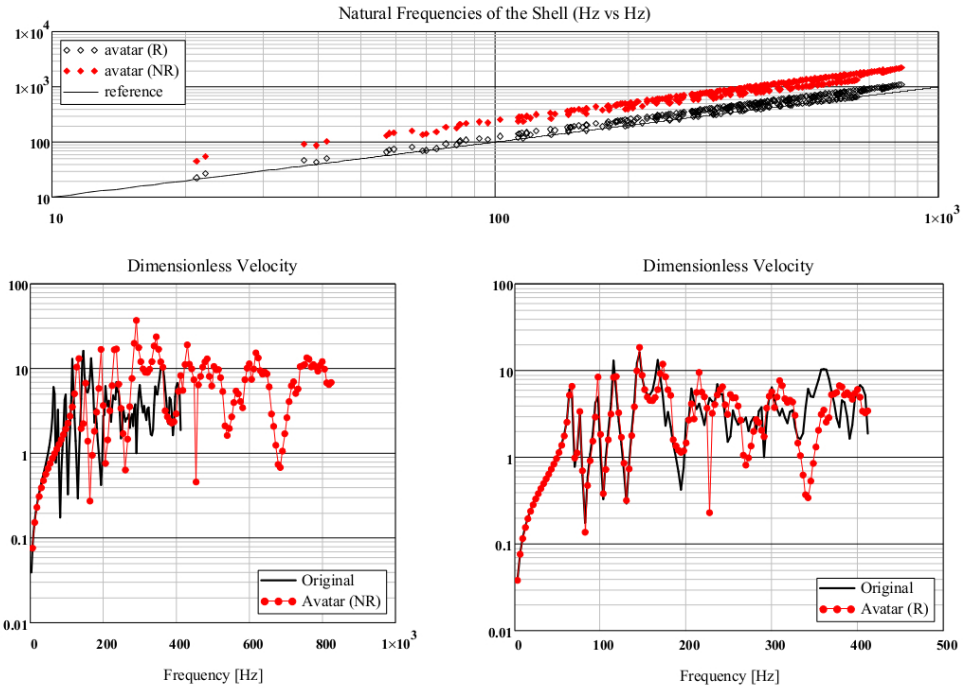

Fig. 9 Stiffened cylinder (L=10 m, R=1 m, h=1 mm, r_L=0.5, r_R=0.5, r_h=1); upper figure: natural frequencies, lower left and right parts: comparisons of the forced responses; avatar: A-Av$_1$S

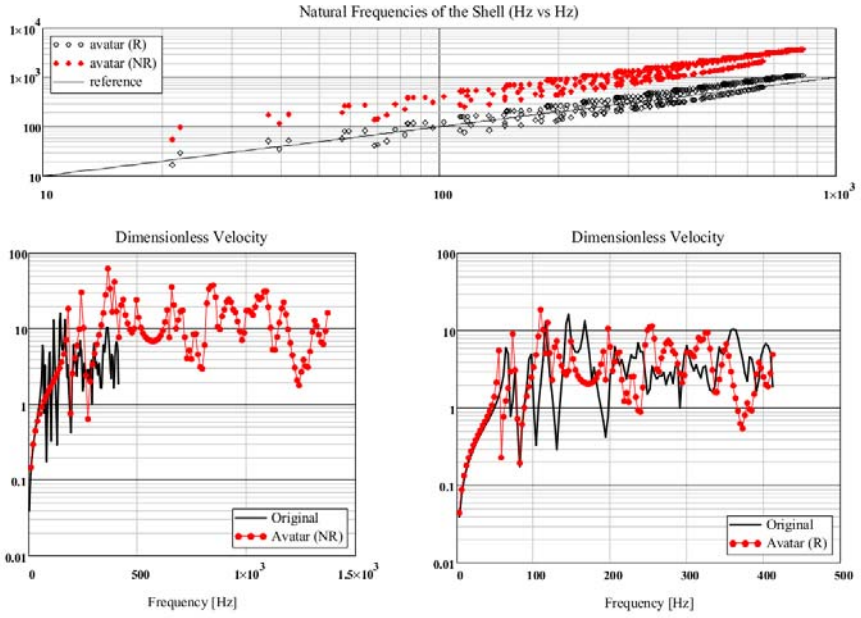

Fig. 10 Stiffened cylinder (L=10 m, R=1 m, h=1 mm, r_L=0.2, r_R=0.2, r_h=1); upper figure: natural frequencies, lower left and right parts: comparisons of the forced responses avatar: A-Av$_2$S

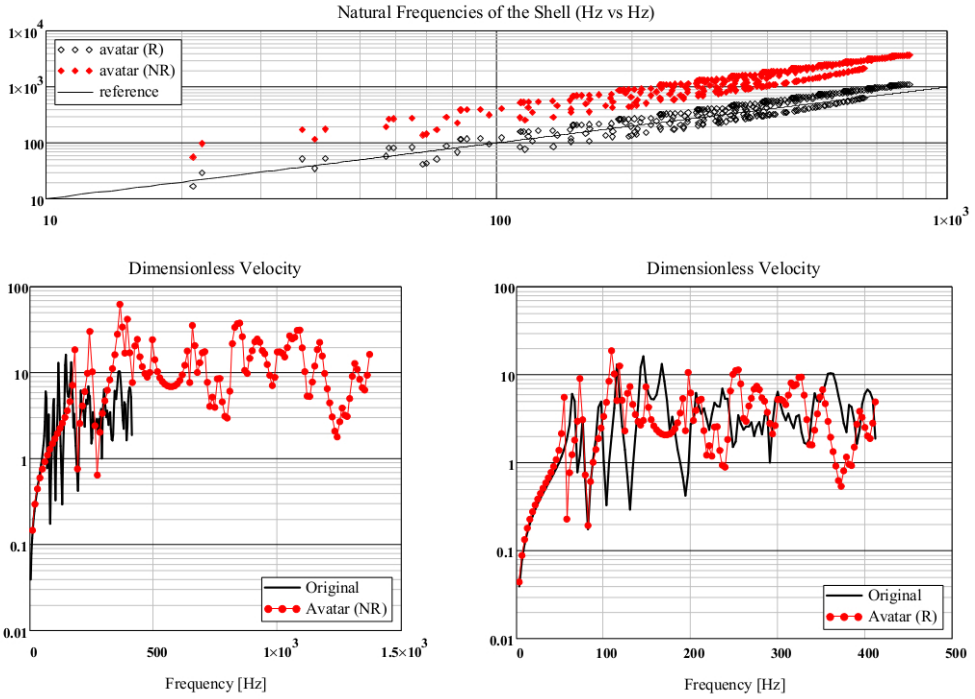

Fig. 11 Stiffened cylinder (L=10 m, R=1 m, h=1 mm, r_L=0.4, r_R=0.3, r_h=0.5); upper figure: natural frequencies, lower left and right parts: comparisons of the forced responses avatar: A-Av$_3$S

Even for these configurations, the results presented in Figs. from 9 to 13 are in the same format used for the unstiffened cases, that is (i) the distribution of the natural frequencies, (ii) the responses before modulation and (iii) after using the scaling laws.

It is useful to firmly precise that the stiffeners in the avatars presented in Table 4 are scaled accordingly with the related directions. This point is later discussed when presenting the final comparisons.

Again, as done before, the A-Av$_1$S, the B-Av$_1$S and C-Av$_1$S allow a joint analysis because they use the same scaling laws. In general, the presence of the stiffeners improves the agreement between the originals and the avatars, Figs. 9, 12 and 13.

In fact, the modal density is lower than the unstiffened cases and the regularity of the modes is broken from the first natural frequencies. Both these considerations emerge form the well-known sequence of modes in the cylindrical shell, Leissa (1973).

As consequence of these effects, it is now difficult to choose the best avatar in this class since all of them replicate rather well the original responses.

The avatar A-Av$_2$S is investigated just to understand the limits of a configuration in which r_L and r_R are largely reduced; from the comparison of Figs. 3 and 10, it is clear that even in an extreme configurations the stiffened cylinder works in an acceptable manner accordingly with the previous considerations.

The avatar A-Av$_3$S is very close to a replica and thus it is able to furnish a good response in a wide frequency range keeping the average of the response and respecting the bounds even with a high degree of distortion.

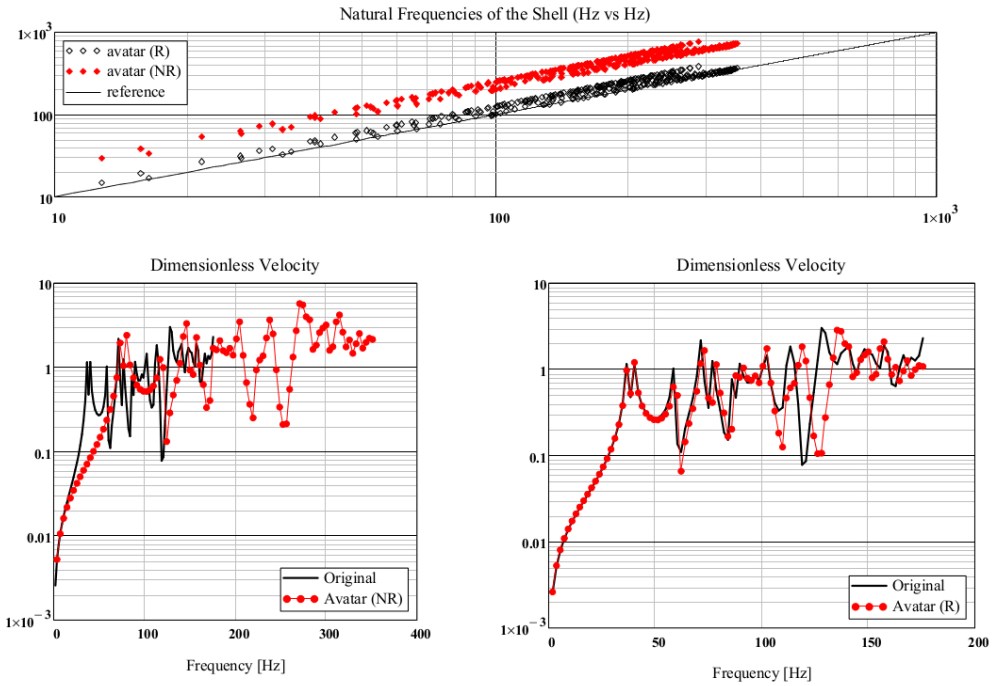

Fig. 12 Stiffened cylinder (L=10 m, R=2 m, h=1 mm, r_L=0.5, r_R=0.5, r_h=1); upper figure: natural frequencies, lower left and right parts: comparisons of the forced responses avatar: B-Av$_1$S

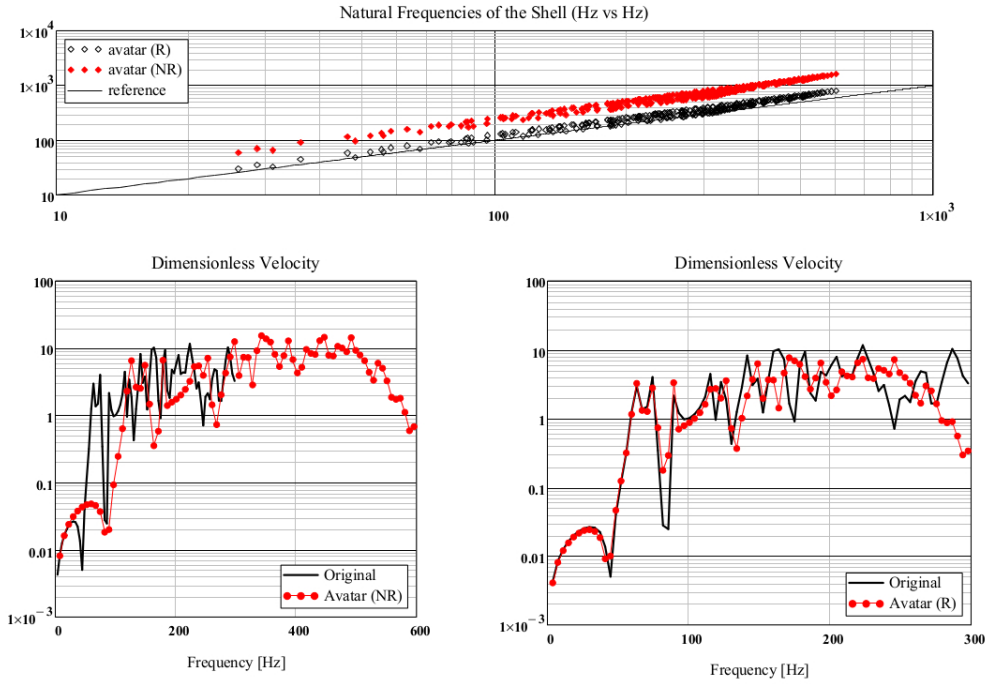

Fig. 13 Stiffened cylinder (L=5 m, R=2 m, h=1 mm, r_L=0.5, r_R=0.5, r_h=1); upper figure: natural frequencies, lower left and right parts: comparisons of the forced responses avatar: C-Av$_1$S

Table 5 Type of avatars

Avatars	r_L	r_R	r_h	NCR, NCL
A-Av$_1$S	0.5	0.5	1	8, 20
B-Av$_1$S				8, 20
A-Av$_1$S-II				4, 10
B-Av$_1$S-II				4, 10

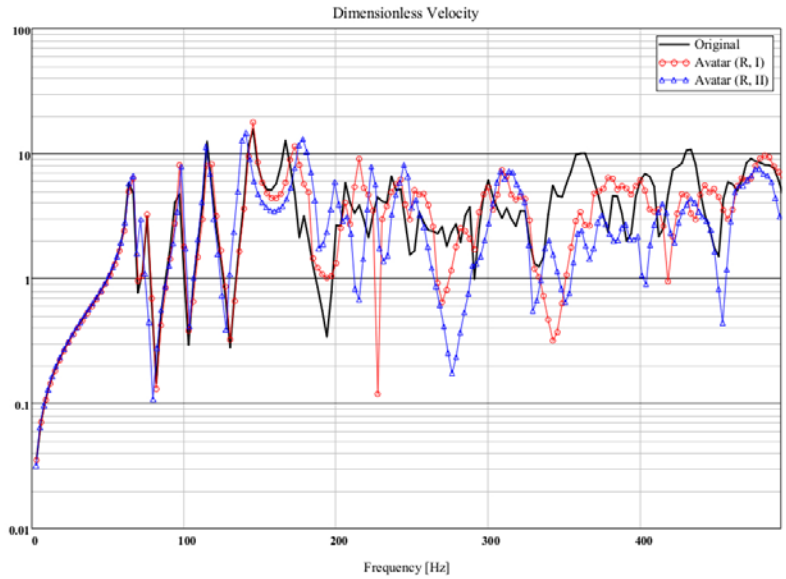

Fig. 14 Stiffened cylinders (L=10 m, R=1 m, h=1 mm, r_L=0.5, r_R=0.5, r_h=1); forced responses; avatars: A-Av$_1$S and A-Av$_1$S-II

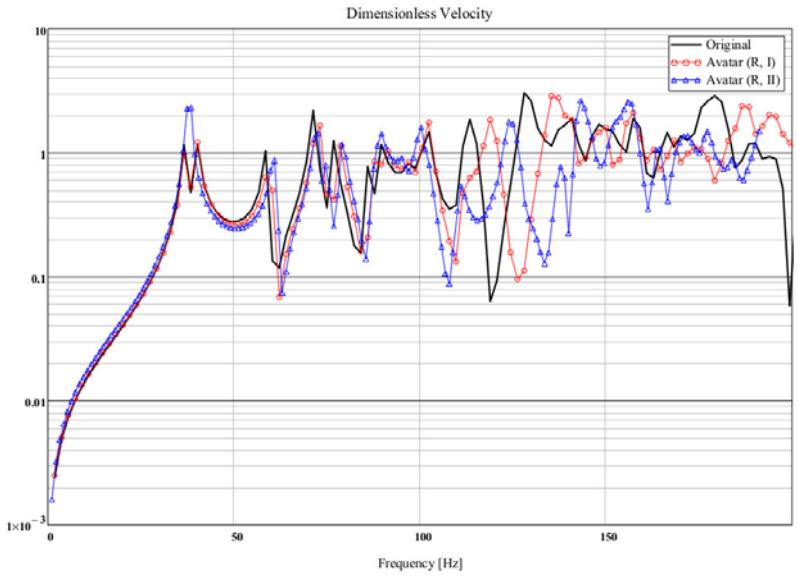

Fig. 15 Stiffened cylinders (L=10 m, R=2 m, h=1 mm, r_L=0.5, r_R=0.5, r_h=1); forced responses avatars: B-Av$_1$S and B-Av$_1$S-II

In all above avatars the areas of the stiffeners are scaled too, according to the scaling laws while the number is kept. This choice can create some manufacturing problems as well as the variation of the thickness in the skins. For this reason the last two charts involve a comparison of the avatars A-Av$_1$S and B-Av$_1$S with another couple of avatars generated by varying the number of the stiffeners and keeping the original areas, Table 5.

Figs. 14 and 15 show the comparison of the original responses for A and B configurations and the related avatars obtained by keeping the number of stiffeners or by keeping their areas (and thus by changing their number).

In both the cases, in the first frequency ranges both the avatars give the same and good results. In presence of local modes, both the avatars represent good approximations of the response in average sense.

7. Conclusions

Some analyses of a similitude for thin cylindrical shells are discussed by using analytical models and the energy distribution approach.

It is investigated the modification of the distribution of the natural frequencies as result of a modification of the length, radius and thickness of the shells. The material and the damping are kept unaltered. The responses of given configurations and the distorted similitude models, named *avatars*, are presented together with the proper scaling laws. The test-case is particularly challenging because the cylindrical shells have a well-known complex sequence of structural modes. The distorted similitudes alter this sequence among longitudinal and circumferential modes.

In the presented case, the attention is concentrated on the possible choices which allow conceiving laboratory models. Thus, configurations with reduced lengths (and radii) are investigated while keeping the original thickness.

It is demonstrated that there is frequency range in which the response of the original and the *avatar* cylinders are the same. The effect of the different choices for the thickness and the length (and radius) parameters influence only the first axial-radial modes.

All results refer to local responses. No average operation is carried out over the structural domain. Therefore, the results are compared versus the highest level of complexity. Any average could smooth the discrepancy between the original and distorted model.

The same quality of the results has been obtained for a stiffened cylindrical shell. In a first set of results, the stiffeners are scaled in longitudinal, radial and circumferential direction according to the analogous laws for the shell. A second set of results is discussed too, in order to simulate a more realistic laboratory condition: the section properties of the stiffeners remain unchanged but their number is changed in a way to keep constant the total section area of the stiffeners.

The results are very encouraging for all presented configurations in view of desired laboratory measurement campaigns. In addition, the configurations with the stiffeners benefit of their stiffening effect of the sequence of the structural modes.

It is useful to underline that the structural model adopted in the present analysis for the stiffened structure is based on the smeared stiffness approach. SAMSARA could be used considering also more complex models, able to detect also local modes since it is based on the modal decomposition. For the same reason even models made with composite materials can be considered. In both the cases, the future tests will reveal the degree of efficacy and accuracy of the avatars.

References

Blevins, R.D. (1987), *Formulas for Natural Frequency and Mode Shapes*, Robert E. Krieger Publishing Company, Melbourne, FL.

De Rosa, S., Franco, F. and Polito, T. (2015), "Partial scaling of finite element models for the analysis of the coupling between short and long structural wavelengths", *Mech. Syst. Signal Pr.*, **52-53**, 722-740.

De Rosa, S., Franco, F. and Polito, T. (2011), "Structural similitude for the dynamic response of plates and assemblies of plates", *Mech. Syst. Signal Pr.*, **25**(3), 969-980.

De Rosa, S., Franco, F., Li, X. and Polito, T. (2012), "A similitude for structural acoustic enclosures", *Mech. Syst. Signal Pr.*, **30** 330-342.

del Rosario, R.C.H. and Smith, R.C. (1996), "Spline Approximation of Thin Shell Dynamics? Numerical Examples", Center for Research in Scientific Computation Technical Report CRSC-TR96-5

Frostig, Y. and Simitses, G.J. (2004), "Similitude of sandwich panels with a soft core in buckling", *Compos. Part B*, **35**, 599-608.

Kline, S.J. (1986), *Similitude and Approximation Theory*, Springer-Verlag, ISBN 0387165185.

Kroes, P. (1989), *Structural Analogies between Physical Systems*, Brit. J. Phil. Scie., **40**, 145-154.

Leissa, A.W. (1973), *Vibration of Shells*, NASA SP-288.

Mace, B.R. (2003), "Statistical energy analysis, energy distribution models and system modes", *J. Sound Vib.*, **264**, 391-409.

Mikulas, M.M. Jr. and McElman, J.A. (1965), "On free vibrations of eccentrically stiffened shells and flat plates", NASA Technical Note D-3010, North Carolina State University.

Rezaeepazhand, J. and Yazdi, A.A. (2011), "Similitude requirements and scaling laws for flutter prediction of angle-ply composite plates", *Compos. Part B: Eng.*, **42**(1), 51-56.

Rezaeepazhand, J., Simitses, G.J. and Starnes, J.H. Jr. (1996), "Design of scaled down models for predicting shell vibration response", *J. Sound Vib.*, **195**(2), 301-311

Rezaeepazhand, J. (2008), "Structural similitude for buckling of delaminated beam", *Key Eng. Mater.*, **385-387**, 609-612.

Singhatanadgid, P. and Songkhla, A.N. (2008), "An experimental investigation into the use of scaling laws for predicting vibration response of rectangular thin plates", *J. Sound Vib.*, **311**, 314-327.

Szucs, E. (1980), *Similitude and Modelling*, Elsevier Science Ltd, ISBN: 0444997806.

Torkamani, Sh., Navazi, H.M., Jafari, A.A. and Bagheri, M. (2009), "Structural Similitude in free vibration of orthogonally stiffened cylindircal shells", *Thin Wall. Struct.*, **47**, 1316-1330.

Wu, J. (2006), "Prediction of the dynamic characteristics of an elastically supported full-size plate from those of its complete-similitude model", *Comput. Struct.*, **84**, 102-114.

Yazdi, A.A. and Rezaeepazhand, J. (2010), "Structural similitude for vibration of delaminated composite beam-plates", *Key Eng. Mater.*, **417**, 742-759.

EC